

## BIOMECHANICAL MULTIBODY MODEL WITH REFINED KINEMATICS OF THE ELBOW

STEPHANIE L. KAHMANN<sup>1,2\*</sup>, STEPHAN USCHOK<sup>2</sup>, KILIAN WEGMANN<sup>2</sup>,  
LARS P. MÜLLER<sup>2</sup> AND MANFRED STAAT<sup>1</sup>

<sup>1</sup>Biomechanics Laboratory, Institute for Bioengineering (IfB)  
Aachen University of Applied Sciences, Heinrich-Mußmann-Str. 1, D-52428 Jülich, Germany  
Stephanie-Lucina.Kahmann@alumni.fh-aachen.de, M.Staat@fh-aachen.de,  
<http://www.ifb.fh-aachen.de/>

<sup>2</sup>Center for Orthopedic and Trauma Surgery, University Medical Center Cologne  
Kerpener Str. 62, D-50937 Köln, Germany  
Stephanie.Kahmann@uk-koeln.de, Stephan.Uschok@uk-Koeln.de, Kilian.Wegmann@uk-koeln.de,  
Lars.Mueller@uk-koeln.de, <https://orthopaedie-unfallchirurgie.uk-koeln.de/>

**Key words:** Biomechanics, Rigid Body Dynamics, Multibody Simulation, Joint Force, Elbow Kinematics, Computational Mechanics.

**Abstract.** The overall objective of this study is to develop a new external fixator, which closely maps the native kinematics of the elbow to decrease the joint force resulting in reduced rehabilitation time and pain.

An experimental setup was designed to determine the native kinematics of the elbow during flexion of cadaveric arms.

As a preliminary study, data from literature was used to modify a published biomechanical model for the calculation of the joint and muscle forces. They were compared to the original model and the effect of the kinematic refinement was evaluated. Furthermore, the obtained muscle forces were determined in order to apply them in the experimental setup. The joint forces in the modified model differed slightly from the forces in the original model. The muscle force curves changed particularly for small flexion angles but their magnitude for larger angles was consistent.

### 1 INTRODUCTION

The range of motion of the elbow plays a crucial role in the activities of daily living [1]. Thus, reducing rehabilitation time after elbow treatment can mean a considerable improvement for patients as well as have an economic impact on the healthcare system. This can be achieved by earlier physiotherapy and less time of the hospital stay.

The elbow has an instantaneous centre of rotation [2], [3] but is simplified as a hinge joint in most models. Furthermore, it is known that a misalignment of an external fixator deviating from the average axis of rotation by only 5° leads to a 3.7-fold increase of energy expenditure in the joint [4]. The higher energy expenditure is covered by increased muscle forces, leading also to higher joint forces. Ignorance of the complex geometry of the elbow might have a comparable effect on the joint force because the instantaneous axis of rotation deviates from the average axis of rotation by several degrees during an arc of flexion from 0° to 90° [2, 3].

External fixators are typically applied after surgical treatments of injuries like traumatic fracture dislocations [5]-[9] or complex interposition arthroplasties [10], in order to provide stabilization and to decrease the joint force [11]. The external fixator allows for early and secure mobilization and rehabilitation. A further decrease of joint force and thus a more physiological movement of the arm might lead to a decrease in rehabilitation duration.

## 2 MATERIALS AND METHODS

In this preliminary study the model arm26.osim by the OpenSim development team (Reinbolt, J., Seth, A., Habib and A., Hamner, S.) was used. The model is based on a published model of Holzbaur et al. [12].

### 2.1 Body Set

The body set includes all needed information about the bones present in the model. This includes the mass and centre of mass of the bones, their moment of inertia around all axes, their geometry as well as their location in dependence of the parent bone, with which it forms a joint. Since the bones are considered to be rigid and no deformation is allowed, no further material properties are required [13]. In the present model, the thorax, the clavicle, the scapula, the humerus, the ulna, the radius and the hand with 36 bones in total are represented with 3 joints to define their position and interaction.

### 2.2 Force Set

The force set defines the properties of force-generating structures (muscles): muscle path, wrap objects, maximum force, fibre length, and tendon slack length amongst others.

The model contains three muscles: triceps muscle, biceps muscle and brachialis muscle, consisting of 6 strands in total. The muscles are defined as the Thelen2003muscle-model, which describes the musculo-tendon behaviour in two nonlinear ordinary differential equations (ODEs) [14]. The first nonlinear ODE describes the activation dynamics, representing a short activation time with a low constant ( $\tau_{act} = 15 \text{ ms}$ ) and a high relaxation time with a high constant ( $\tau_{deact} = 50 \text{ ms}$ ) [15].

$$\frac{da}{dt} = \frac{u - a}{\tau_a(a, u)}$$

where  $u$  is an idealized muscle excitation signal and is related to  $a$ , being the muscular activation. The time constant  $\tau_a$  depends on the muscle activation level and can be set to  $\tau_{act}$  for the activating phase or  $\tau_{deact}$  for the deactivating phase of the muscle contraction:

$$\tau_a(a, u) = \begin{cases} \tau_{act} (0.5 + 1.5a); & u > a \\ \frac{\tau_{deact}}{(0.5 + 1.5a)}; & u \leq a \end{cases} \quad (2)$$

Equation (2) reflects an increase in activation time with higher activation level, whereas the deactivation time increases with lower activation level. The given behaviour is associated with the increasing presence of calcium during activation and the decreasing presence of calcium

during deactivation [15].

The other nonlinear ODE reflects the activation of the force-generating musculo-tendon actuator [16]. It expresses the relation between the force, length and velocity of the muscle to the elastic properties of the tendon.

$$V^M = \frac{d\bar{L}^M}{dt} = (0.25 + 0.75a)V_{\max}^M \frac{\bar{F}^M - ae^{-\frac{-(\bar{L}^M - 1)^2}{\gamma}}}{b} \quad (3)$$

Here  $V^M$  is the contraction velocity,  $\bar{L}^M$  as the normalized muscle fiber length,  $V_{\max}^M$  is the maximal contraction velocity,  $\bar{F}^M$  is the normalized active muscle force,  $\gamma$  as a shape factor accounting for the force-length relationship, and  $b$  is a parameter, which is defined differently for shortening or lengthening of the muscle (see Eq. 4, [14]):

$$b = \begin{cases} af_l + \frac{\bar{F}^M}{A_f}; & \bar{F}^M \leq af_l \\ \left(2 + \frac{2}{A_f}\right) \frac{(af_l \bar{F}_{len}^M - \bar{F}^M)}{\bar{F}_{len}^M - 1}; & \bar{F}^M > af_l \end{cases} \quad (4)$$

with  $f_l$  being an active force-length scale factor,  $\bar{F}_{len}^M$  being the maximal normalized muscle force when lengthening and  $A_f$  being a force-velocity shape factor. With following equation, the force on the bone is described:

$$F^T = F^{MT} = F_0^M \bar{F}^T (\varepsilon^T) \quad (5)$$

with  $F^T$  being the force which the tendon applies on the bone and which is generated by the muscle-tendon compound  $F^{MT}$ . It consists of the maximum isometric muscle force  $F_0^M$  and the normalized force in the tendon  $\bar{F}^T$  with respect to the maximum isometric muscle force and depends on the tendon strain  $\varepsilon^T$  [17]. This leads to

$$F^{MT}(t) = F_0^M \begin{cases} \frac{\bar{F}_{toe}^T}{e^{k_{toe} \varepsilon^T} - 1} \left( e^{\frac{k_{toe} \varepsilon^T}{\varepsilon_{toe}^T}} - 1 \right); & \varepsilon^T \leq \varepsilon_{toe}^T \\ k_{lin} (\varepsilon^T - \varepsilon_{toe}^T) + \bar{F}_{toe}^T; & \varepsilon^T > \varepsilon_{toe}^T \end{cases} \quad (6)$$

where  $\varepsilon_{toe}^T$  stands for the tendon strain in the toe region and above which the strain behaves linearly. The corresponding normalized tendon force is  $\bar{F}_{toe}^T$ .  $k_{toe}$  and  $k_{lin}$  are an exponential shape factor and a linear scale factor, respectively.

The relation of the normalized fibre length and the active force-length scale factor is described as:

$$f_l = e^{-\frac{-(\bar{L}^M - 1)^2}{\gamma}} \quad (7)$$

All parameters are adjusted so that the muscles show the behaviour for muscles in healthy

older adults. This includes an adjustment of the relaxation time, which is longer compared to muscles in young adults. Furthermore, the maximum torques, achieved in lengthening, isometric and shortening contractions were decreased and the estimated times to reach 50 % of maximum torque were increased in this muscle model to represent the behaviour for muscles in old males compared to young males in the Hill-type muscle model [13].

### 2.3 Modifications

In this strongly simplified model, the elbow hinge joint was exchanged for a custom-designed joint. Thus, the fixed axis was exchanged for an axis, which translates along and rotates around two axes, respectively. The data from literature [2] was processed and inserted, so that the flexion axis moved translationally in two dimensions by 1.4 mm and 2 mm, respectively, as well as rotationally around two axes by  $5.7^\circ$  and  $2.6^\circ$ , respectively, as a function depending on the flexion axis. As the average axis of rotation was distal compared to the hinge joint axis of the original model, the slack-lengths of the muscles crossing the elbow joint were adjusted. These modifications were evaluated by comparing the muscle forces of both, the original and the modified model.

### 2.4 Computed Muscle Control

A calculation of the joint forces and muscle forces was performed, using the computed muscle control (CMC) tool of OpenSim. In the tool, the kinematics of a model is defined either by experimental data from experiments or by a data set for joint angles. In this study, a data set, defining an elbow flexion from  $0^\circ$  to  $90^\circ$  was used.

The tool aims for muscle excitations that lead to the specified kinematics in a forward dynamic simulation [18].

Firstly, the current position of the model is calculated by decreasing the difference in marker distance or in coordinate values of the desired and given state. That calculation also includes the current muscle activation levels and muscle fiber lengths. From that, the accelerations can be found with the following proportional derivative equation:

$$\ddot{\vec{q}}^*(t+T) = \ddot{\vec{q}}_{\text{exp}}(t+T) + k_v[\dot{\vec{q}}_{\text{exp}}(t) - \dot{\vec{q}}(t)] + k_p[\vec{q}_{\text{exp}}(t) - \vec{q}(t)] \quad (8)$$

with  $\ddot{\vec{q}}^*$  as the desired accelerations,  $\ddot{\vec{q}}_{\text{exp}}$  as the experimental accelerations,  $\dot{\vec{q}}_{\text{exp}}$ ,  $\dot{\vec{q}}$ ,  $\vec{q}_{\text{exp}}$  and  $\vec{q}$  as the experimental and simulated velocities and positions, respectively, and  $k_v$  and  $k_p$  as the feedback gains for the velocity and position errors [19]. With the solution of this equation, the tool finds the muscle excitations required to evoke the found accelerations. The distribution of forces between the muscles is found using static optimization, aiming to minimize the metabolic energy. Therefore, the forces are distributed with the factor of their maximum force. With these newly adjusted muscle forces, a forward dynamic simulation is carried out, in order to find the corresponding velocities and accelerations [20].

## 3 RESULTS

The first question we aimed to answer was if the refinement of the joint kinematics has an impact on the joint force. Therefore, the results of the CMC tool were analysed. The joint forces are given in the ground coordinate system as shown in Figure 1.

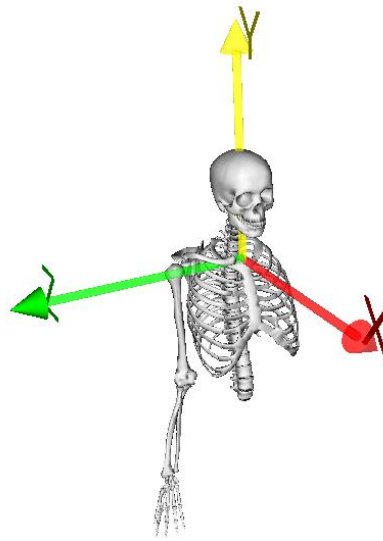


**Figure 1:** The ground coordinate system showing the coordinate system in which the joint forces are given.

The joint reaction force of the model from the OpenSim development team was compared to the one of the modified model when doing the same motion, an elbow flexion from  $0^\circ$  to  $90^\circ$ .

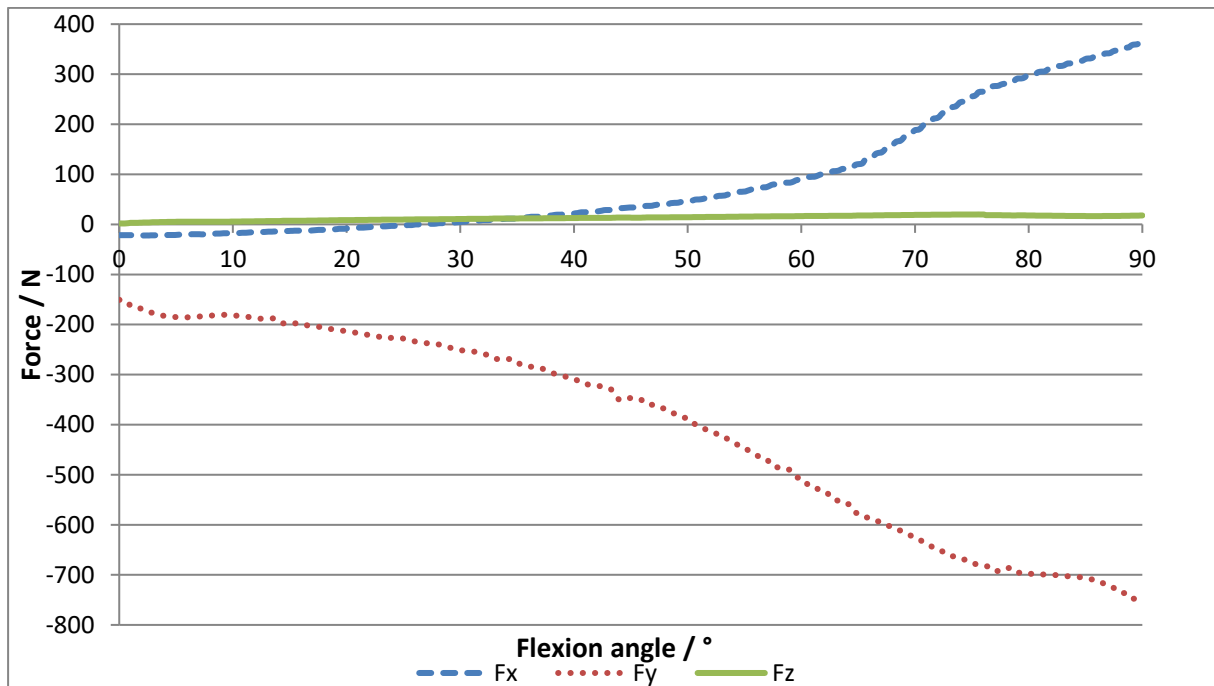


**Figure 2:** Components of the joint reaction force over the flexion angle of the arm26.osim model.

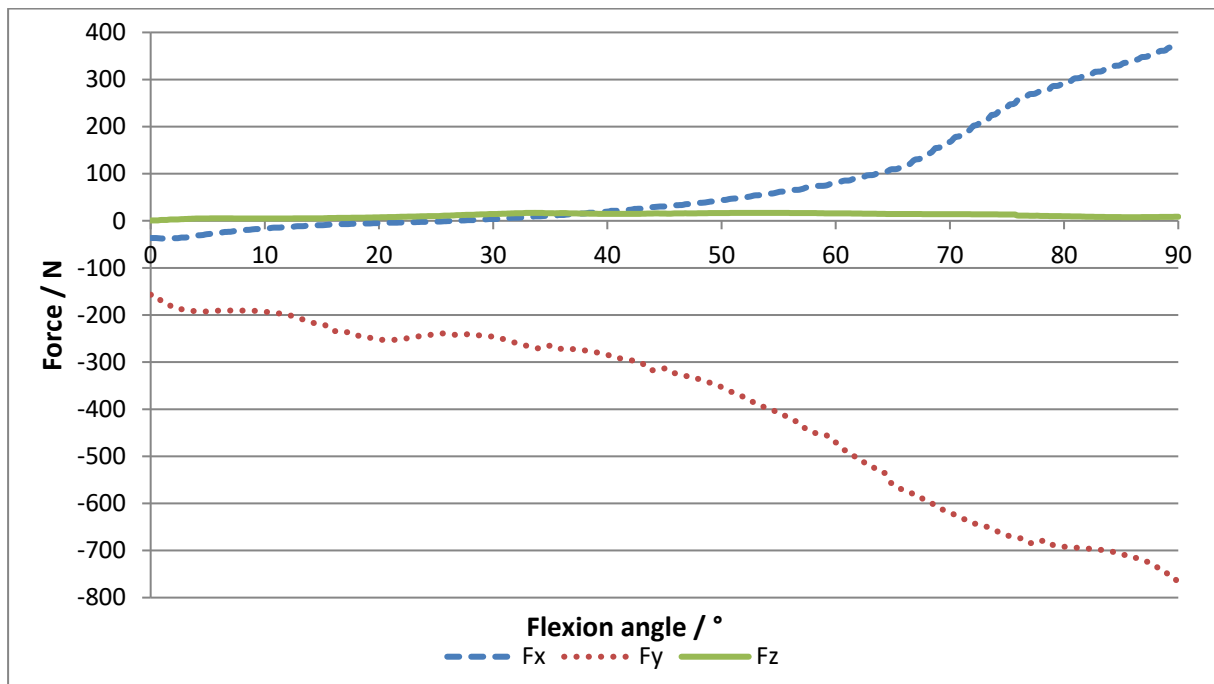


**Figure 3:** Components of the joint reaction force over the flexion angle of the modified model.

In both models the maximum joint reaction force occurs at full extension in the negative y-direction and reaches up to around 780 N. For flexion angles between 10° and 35°, the modified model shows higher forces in negative y-direction. In 20 ° flexion the original model shows a force of 212 N whereas the modified model shows a force of 252 N.

The second biggest joint reaction force points into positive x-direction and reaches up to 380 N in both models.

Furthermore, it was important to prove that the muscle forces remain in the physiological range and behaviour. Therefore, the muscle forces were reviewed (see Figures 4 and 5). The paths of the triceps muscle strands can be seen in Figure 4, the paths of the brachialis and biceps muscle strands in Figure 5.

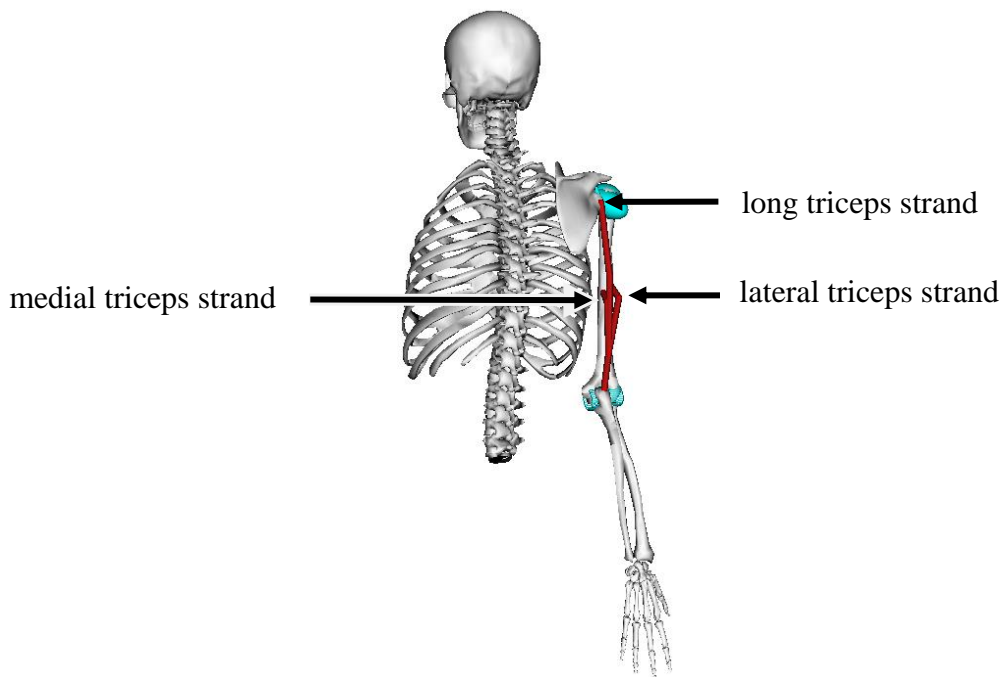


**Figure 4:** Muscle paths of the long, medial and lateral strand of the triceps muscle from ventral view.

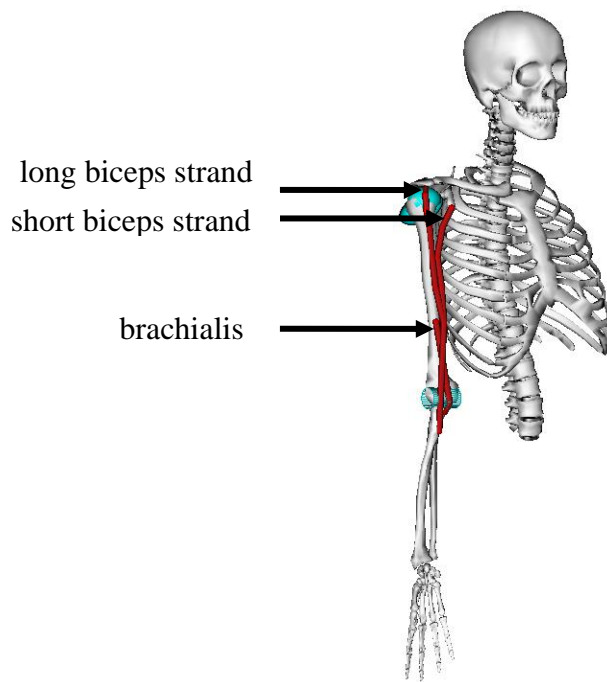


**Figure 5:** Muscle paths of the brachialis and the long and short strand of the biceps muscle.

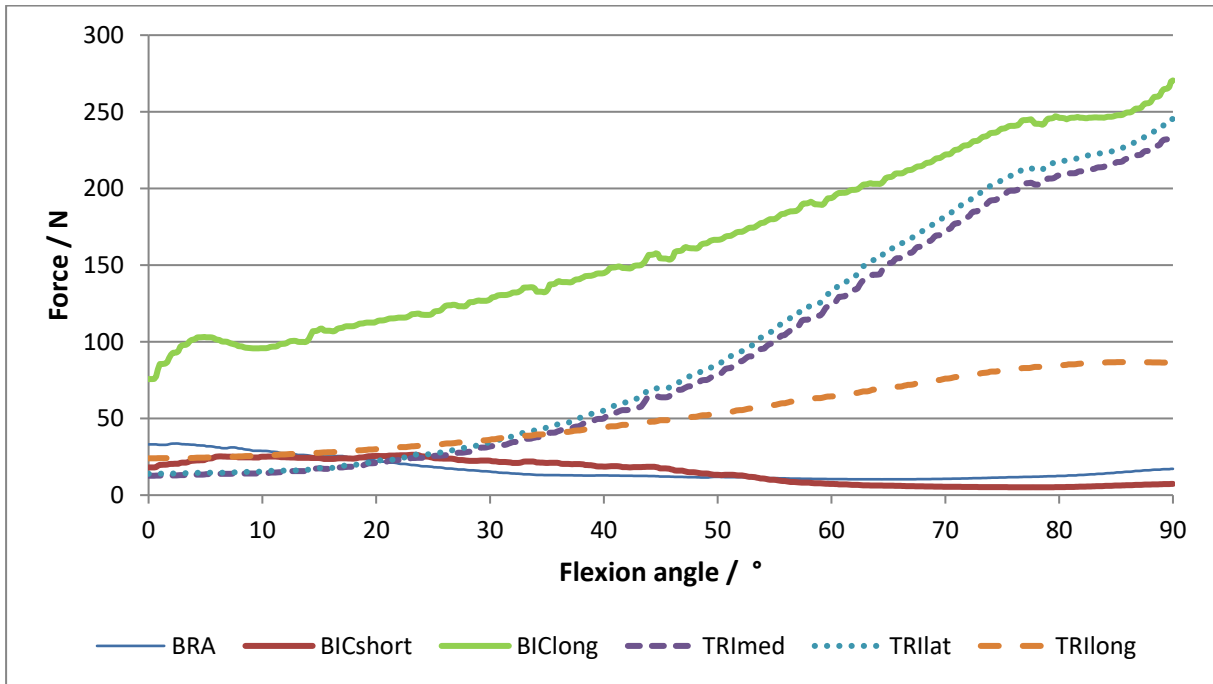


**Figure 6:** Muscle forces of the original model in dependence of the flexion angle.

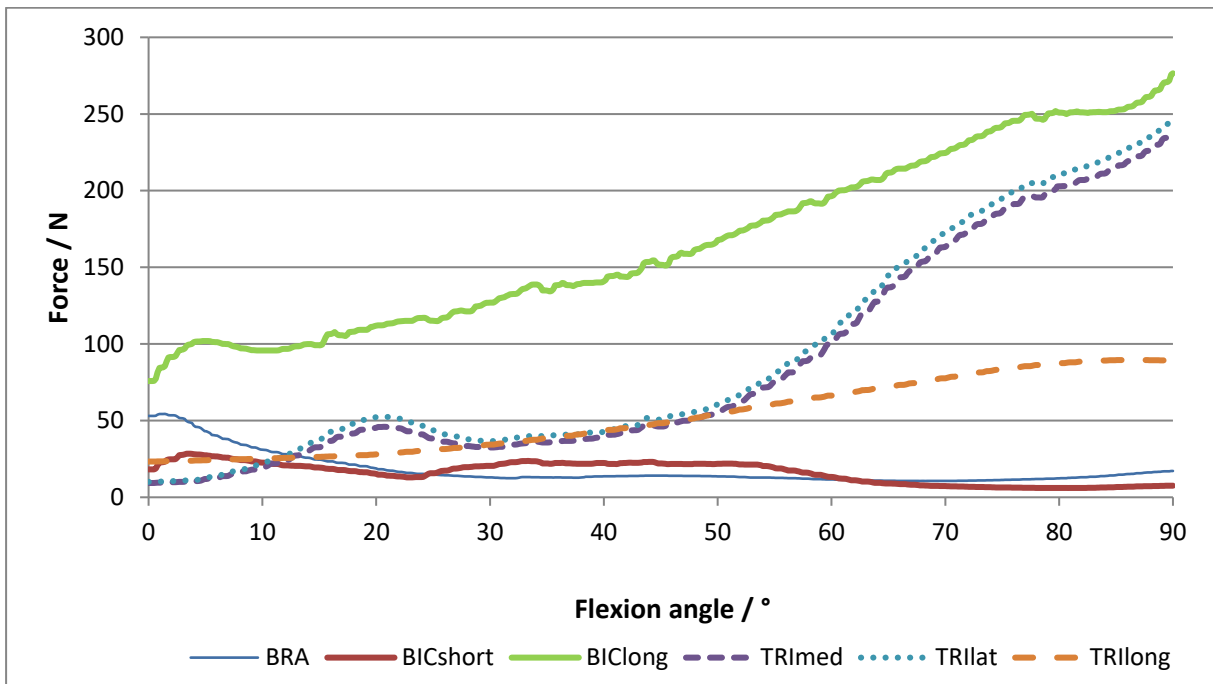


**Figure 7:** Muscle forces of the modified model in dependence of the flexion angle.

It can be seen that the muscle forces remain in their physiological range and behaviour. In both models the biceps muscle applies the highest force, particularly with its long strand. The maximum force in both models comes to around 275 N in 90° flexion. The biggest difference

can be observed in the muscle forces of the medial and lateral strand of the triceps muscle from 5° to 30° flexion. In 20° of flexion, the lateral triceps strand applies 20.5 N in the original and 52.5 N in the modified model.

#### **4 DISCUSSION**

The current model was a preliminary study with the aim to find out if further research is requested. That was proven with the change in joint forces. The most important differences between the models can be observed in the y-direction, which points from distal to proximal, in the range between 10° and 35° of flexion. This component accounts for the direction, which all muscles have in common and increases the compression force in the joint. It can be proposed, that this increase might be due to the medial and lateral strand of the triceps muscle, as they also show an increase in that range of flexion, in comparison to the original model. That might be due to a lower stability provided by the bones in the lower flexion, which is compensated by these two muscle strands. This is supported by the fact, that the muscle paths of these strands allow stabilization to the medial and lateral side.

The second biggest force points into anterior direction and is required for the flexion motion.

Different courses in the joint reaction forces suggest that a newly designed external fixator, following closely the joint kinematics, can also decrease the joint force.

However, although considerable changes in the kinematics were made, the muscle forces remained physiologically, which indicates, that the findings are reliable. The information about the muscle forces can now be implemented into the experimental setup in order to come closer to the physiological conditions.

#### **5 OUTLOOK**

The presented preliminary results are the basis for further research for which an experimental setup with a robot is created. The proximal part of a humerus of a human cadaveric arm is potted into resin, which is fixed in an upper jig, the distal part is also potted into resin, which is connected to a force torque sensor (FTN Mini 45, Schunk GmbH & Co. KG, Lauffen am Neckar, Germany). This sensor is attached to the tip of a robot arm (Epson ProSix S5-A701S, Seiko Epson Corporation, Suwa, Nagano, Japan) and a marker of an optical tracking system (Optotrak Certus Motion Tracking System, NDI Northern Digital Inc., Waterloo, Ontario, Canada) is pinned to the cadaveric arm. The triceps, biceps and brachialis muscles will be pulled in the manner this preliminary study showed.

The control of the robot as well as the sensor and the optical tracking system are programmed in C++. The robot moves the arm from 0° to 90° of flexion while the force torque sensor measures forces and torques corresponding to 6 degrees of freedom. If the measured forces and exceed specified thresholds, the software requests a change in position of the robot so that the robot moves the arm into the direction of decreasing force or torque. Thus, the robot moves the cadaveric arm along the path of smallest resistance taking the radius of the flexion as well as the pronation-supination angle and the varus-valgus angle into account. The found path is assumed to be the physiological path of the elbow flexion. The positions considered to be the physiological position for every degree of flexion are tracked with the optical tracking system and the software saves their coordinates

A first preliminary experimental study showed the possibility to gain the sought data but

some modifications are required before experiments can be performed.

The experimental data can be implemented into a more detailed biomechanical multibody model with more muscles. It will be modified using the experimentally collected data so that reliable results can be obtained.

## 6 ACKNOWLEDGEMENTS

This study was supported by Prof. Jeffrey A. Reinbolt, University of Tennessee, Knoxville, who helped to estimate the model capabilities, on which the preliminary study is based and helped to evaluate the results of the computed muscle control tool by OpenSim and who gave consultation for the development of the model.

Furthermore, the ECCOMAS Scholarship of the ECCOMAS Managing board is very much appreciated, which allows the presentation of the study at the 6<sup>th</sup> European Conference on Computational Mechanics (ECCM 6).

## REFERENCES

- [1] Bryce, C. D. and Armstrong, A. D. Anatomy and biomechanics of the elbow. *Orth. Clin. N. Am.* (2008) **39**(2): 141-154.
- [2] Bottlang, M., Madey, S. M., Steyers, C. M., Marsh, J. L., and Brown T. D. Assessment of elbow joint kinematics in passive motion by electromagnetic motion tracking. *J. Orthop. Res.* (2000) **18**(2): 195-202.
- [3] Ericson, A., Arndt, A., Stark, A., Wretenberg, P., and Lundberg, A. Variation in the position and orientation of the elbow flexion axis. *J. Bone Joint Surg.* (2003) **85**(4): 538-544.
- [4] Madey, S. M., Bottlang, M., Steyers, C. M., Marsh, J. L., and Brown, T. D. Hinged external fixation of the elbow: optimal axis alignment to minimize motion resistance. *J. Orthop. Trauma* (2000) **14**(1): 41-47.
- [5] Cobb, T. K. and Morrey, B. F. Use of distraction arthroplasty in unstable fracture dislocations of the elbow. *Clin. Orthop. Relat. R.* (1995) **312**: 201-210.
- [6] Ruch, D. S. and Triepel, C. R. Hinged elbow fixation for recurrent instability following fracture dislocation. *Injury.* (2001) **32**: 70-78.
- [7] Lee, D. H. Treatment options for complex elbow fracture dislocations. *Injury.* (2001) **32**: 41-69.
- [8] Zilkens, C., Graf, M., Anastasiadis, A., Smajic, S., Muhr, G., and Kälicke, T. Treatment of acute and chronic elbow instability with a hinged external fixator after fracture dislocation. *Acta Orthop. Belg.*(2009) **75**: 167-174.
- [9] Nestorson, J., Josefsson, P.-O., and Adolfsson, L. A radial head prosthesis appears to be unnecessary in Mason-IV fracture dislocation. *Acta Orthop.* (2017) **88**(3): 315-319.
- [10] Nandi, S., Maschke, S., Evans, P. J., and Lawton, J. N. The stiff elbow. *Hand.* (2009) **4**: 368-379.
- [11] Bigazzi, P., Biondi, M., Corvi, A., Phanner, S., Checcucci, G., and Ceruso, M. A new autocentering hinged external fixator of the elbow: A device that stabilizes the elbow axis without use of the articular pin. *J. Shoulder Elb. Surg.* (2015) **24**(8): 1197-1205.
- [12] Holzbaur, K. R. S., Murray, W. M., and Delp, S. L. A model of the upper extremity for

- simulating musculoskeletal surgery and analyzing neuromuscular control. *Ann. Biomed. Eng.* (2005) **33**(6): 829-840.
- [13] Verjans, M. R., Siroros, N., Eschweiler, J., and Radermacher, K. M. Technical concept and evaluation of a novel shoulder simulator with adaptive muscle force generation and free motion. *Current Directions in Biomedical Engineering* (2016) **2**: 61-65.
- [14] Thelen, D. G. Adjustment of muscle model parameters to simulate dynamic contractions in older adults. *J. Biomech. Eng.- T. ASME.* (2003) **125**(1): 70-77.
- [15] Winters, J. M. An improved muscle-reflex actuator for use in large-scale neuromusculoskeletal models. *Ann. Biomed. Eng.* (2005) **23**: 359-374.
- [16] Zajac, F. E. Muscle and tendon: Properties, models, scaling and application to biomechanics and motor control. *Crit. Rev. Biomed. Eng.* (1989) **17**: 359-411.
- [17] John, C. T., Anderson, F. C., Higginson, J. S., and Delp, S. L. Stabilization of walking by intrinsic muscle properties revealed in a three-dimensional muscle-driven simulation. *Comput. Methods Biomech. Biomed. Engin.* (2013) **16**(4): 451-462.
- [18] Delp, S. L., Anderson, F. C., Arnold, A. S., Loan, P., Habib, A., John, C. T., Guendelman, E., and Thelen, D. G. OpenSim: open-source software to create and analyze dynamic simulations of movement. *IEEE Trans. Biomed. Eng.* (2007) **54**(11): 1940-1950.
- [19] Thelen, D. G. and Anderson, F. C. Using computed muscle control to generate forward dynamic simulations of human walking from experimental data. *J. Biomech.* (2006) **39**(6): 1107-1115.
- [20] Birgel, S., Leschinger, T., Wegmann, K., and Staat, M. Calculation of muscle forces and joint reaction loads in the shoulder area via an OpenSim based computer model. *Tech. Mess.* (2018).